PROCEEDINGS, 50th Workshop on Geothermal Reservoir Engineering
Stanford University, Stanford, California, February 10-12, 2025
SGP-TR-229

Hydraulic Fractures Are Pressure Relief Valves

Luke P. Frash

Los Alamos National Laboratory, PO Box 1663, Los Alamos, NM 87545

lfrash@lanl.gov

Keywords: Concepts, Frac Gradient, Stress Dependent Permeability, Mechanics

ABSTRACT

Sometimes, it is helpful to question and revisit our conceptual understanding of how processes work rather than rely on complex coupled simulations that incorporate ever-more physics and complexity. This is especially true for hydraulic fracturing because it involves a system with exceptionally high uncertainty which then limits the utility of having precise physics calculations. It is also true when the application scope changes for the technology, such as transitioning from oil and gas (O&G) to enhanced geothermal systems (EGS). Conceptually, hydraulic fracture initiation and extension requires injecting fluid into a well at a sufficiently high rate that the pressure reaches the limit required for tensile opening. If the injection rate increases beyond this limit, the typical assumption will be that pressure will continue to rise. However, the actual behavior is more interesting and potentially quite useful for geothermal applications. In this study, we elucidate how injection pressures behave as flow rate is increased from zero to ludicrous speed to show how hydraulic fractures can be thought of as functionally akin to pressure relief valves. We then discuss how this concept can help to understand fracture behavior in EGS and what this could mean for its technological viability.

1. INTRODUCTION

Our understanding of hydraulic fracture mechanics has advanced significantly over the past seven decades (Hubbert and Willis, 1957; Valko and Economides, 1996; Zoback, 2010). The emphasis of this study topic has been to answer questions regarding fracture orientation, length, aperture, and height growth (Perkins and Kern 1961; Geertsma and De Klerk, 1969; Nordgren, 1972; Fisher and Warpinski, 2012). The key concerns being the risk of inadvertent aquifer contamination from hydraulic fracturing fluid and achieving more production from unconventional oil and gas wells. These advancements focused on increasing our ability to model complexity, improving computational capabilities, leveraging high-performance computers, and integrating ever-more sources of data (Lecampion et al., 2018). This approach has proven its merit for developing unconventional shale oil and gas plays using techniques such as multi-stage completions with directional drilling. Recently, a new milestone was achieved by transitioning this learning to geothermal energy at Blue Mountain, where multi-stage hydraulic fracturing completions were implemented in a hot dry rock environment (Norbeck and Latimer, 2023). However, the optimal method for developing deep geothermal resources remains a topic of ongoing research and development. High-level tools are needed to assure that time, effort, and resources are committed to the most promising methods and to avoid misinterpretation of the results from the new and novel methods that are being proposed and tested as we collectively seek to develop geothermal resources.

For this study, my goal is to clarify concepts regarding the signatures of subsurface phenomena that can be identified from injection well data. More specifically, I show how injection pressure and injection rate are related and then I discuss the implications of this relationship. Understanding the fundamentals of this concept helps to more accurately interpret the signature of tensile fracture opening, the meaning of injectivity and inferred fracture permeability, and implications for reservoir behavior. This is especially important as new tools such as machine learning (ML) and artificial intelligence (AI) gain popularity, because these tools can create false confidence. Our fundamental understanding is needed to verify their output. In this study, I present a simple model to predict the behavior of an injection well that is based on my experience completing laboratory and field hydraulic fracturing experiments in crystalline rock and rock analogs (Frash et al., 2015; Frash et al., 2019; Frash et al., 2021; Frash et al., 2025; Kneafsey et al., 2025; Madenova et al., 2025). Then I discuss why a more accurate understanding of these concepts could be beneficial for a variety of newly proposed concepts and for interpreting the results of injection tests into geothermal wells. Ultimately, a takeaway message from this paper is to introduce the concept that hydraulic fractures are functionally identical to a leaky pressure relief valve.

2. A CONCEPTUAL MODEL

It is possible to harvest the heat from deep hot dry rock (HDR; Brown et al., 2012) using a combination of injection wells, fractures, and production wells – a concept referred to as enhanced geothermal systems (EGS). The existence of many complex and sophisticated models available to simulate these systems does not mean that a simple model cannot suffice to gain a better understanding of how they work. On the contrary, a simple model can offer a more direct path to conceptual understanding, so that is what we will do here. First, let us consider the EGS concept and an analogous hydraulic circuit (Figure 1). If we take note of symmetry, the system can even be modeled as a series circuit with flow passing through the injection well, out through the constricted near-well zone, through fractures, and then collected via a production well that is purposely intersecting the stimulated fracture network. Our question requires considering the pressure-dependent flow behavior through this circuit as the injection rate is ramped up from zero to ludicrous speed. The profile of this relationship will show how the non-linear behavior of fractures as pressure increases yields a unique signature in timeseries data. This signature is not intuitive without first understanding the concepts detailed here.

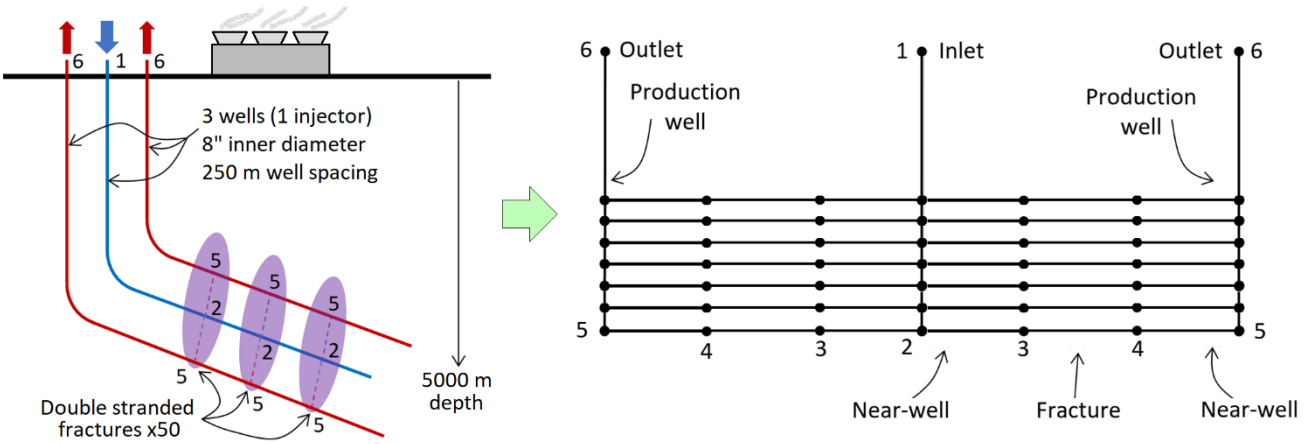

Figure 1: The EGS concept can be conceptually represented as a hydraulic circuit of pipes and nodes with each having properties that are representative of the underground heat exchange system. In this study, we will focus only on hydro-mechanical effects that have a direct influence on injection well flow and pressure behavior.

Next, let us outline some key equations for the flow through pipes and fractures. For pipes (x), we use Hazen-Williams (Jeppson, 1974) with pipe that is assumed to be so highly corroded (f) that the imprecision of this model is irrelevant. For fractures, we will forego the norm of using fracture permeability (k) and instead use effective hydraulic aperture (h) because it is more directly scalable to fractures of different sizes and it requires fewer assumptions to apply. Furthermore, hydraulic aperture is based on cubic law so it is crucial to recognize that it's dimension will be factorially (N) different from mechanical aperture (Ψ) – i.e., the physical size of the fracture's opening which is sometimes alternatively referred to as fracture width (Witherspoon et al., 1980). The pressure drop (ΔP) induced by flow (Q) in the near well region will be dominantly radial (r; Yen, 1962) whereas the flow further afield will be dominantly linear (l), so two relationships for fracture flow are needed. After toying around with these equations in series flow, I found that a ratio of 1:6 between well spacing (L), and the effective radius of radial flow (r) seemed reasonable. Likewise, the linear fracture flow length (l) can be taken as roughly equal to the flow height (H). This gives a system of equations that can now be solved when given an appropriate fluid viscosity (μ) and selected well hydraulic radius (R_w).

$$\Delta P_x = \frac{1.14\times10^8 Q^{1.852}\mu x}{f^{1.852}(2R_w)^{4.87}} \tag{1}$$

$$\Delta P_l = \frac{12Q\mu l}{Hh^3} \tag{2}$$

$$\Delta P_r = \frac{6Q\mu \ln(r/R_w)}{\pi h^3} \tag{3}$$

$$l \approx \frac{2}{3}L \tag{4}$$

$$r \approx \frac{1}{6}L \tag{5}$$

$$k = \frac{h^3}{12\Psi} \tag{6}$$

$$h = N\Psi \tag{7}$$

In addition, we can consider the stress-dependency of fracture aperture (Li et al., 2021; Welch et al., 2022; Meng et al., 2021), for which I prefer to use a scalable exponential relationship as a function of fracture compressibility (α) and normal effective compressive stress (σ_n') when the facture is held closed by rock stress. Per Terzaghi's principles for a well-connected hydraulic interface, effective stress is a function of only pore pressure (p) and total stress (σ_n). In the case of vertical hydraulic fractures, the normal stress can be estimated from a passive earth stress coefficient (K) of 0.5 because the prospective stress field will preferably be normally faulted with gravitational (g) overburden as a function of mean rock density (ρ) and depth (D).

$$\Psi' = \Psi_0 e^{-\alpha\sigma_n'} \tag{8}$$

$$\sigma_n' = \sigma_n - p \tag{9}$$

$$\sigma_n = K\rho g D \tag{10}$$

When the injection pressure becomes high enough for the fracture to be held open by fluid pressure, the aperture becomes a function of net fluid pressure (P_n), fracture radius (R_f) and elastic moduli (E and v). This introduces an abrupt change in the flow dynamics because the permeability of an open fracture can be orders of magnitude higher than a closed fracture.

$$\Psi = \frac{8P_n(1-\nu^2)R_f}{\pi E} \tag{11}$$

Next, let us assume that we know the critical pressure (P_n) at which a hydraulic fracture will begin to grow so that we can solve for the fracture apertures at which the radius of a fracture will remain constant. This is important for fractures that are intended to be stable over time, such as for EGS along with caged geothermal systems (CGS) or geopressured geothermal systems (GGS). During this time, the fractures will have a hydraulic conductivity that is capable of being substantially higher than that of the wells, so the well sizes become the key limiting factor for flow rate as a function of pressure. This concept is central to the analogy between a hydraulic fracture and a pressure relief valve: the injection pressure is capped by the normal stress acting on the factures combined with the pressure relieving flow from the production wells.

$$P_n = P_c \tag{12}$$

Fracture propagation will resume only if the injection rates reach ludicrous speeds with respect to what the production wells can support. At very high flow rates, the backpressure from the production wells can become so high that the fractures will propagate. We regard this point as the fracture caging limit and the upper limit for injection into an EGS reservoir given its goal to maintain long-term production with minimal fluid losses and minimal risk of injection induced seismicity. In the next section, we evaluate these flow limits using the above equations solved within the context of the hydraulic circuit. Note that our solution uses the iterative solvers provided on our data repository (Frash et al., 2023).

3. MODEL PARAMETERS

The base case for our model assumes the parameters as presented in Table 1. Note that we include variables for the number of hydraulic fractures and the number of strands that the hydraulic aperture of each fracture is distributed among. This information is compounded into the effective hydraulic aperture for the model to account for multi-stage stimulation and fracture complexity. Radial flow terms and flow rate terms for the production wells are proportioned by the number of those wells to maintain equal flow balance.

$$h' = \sqrt[3]{\left(n_f n_s \left(\frac{h}{n_s}\right)^3\right)} \tag{13}$$

Table 1: Model Parameters

Parameter	Value	Symbol	Parameter	Value	Symbol
Production Wellhead Pressure Head	5.0 MPa	P_6	Fluid Viscosity	0.2 cP	μ
Production Bottomhole Pressure Head	-	P_5	Fluid Density	958 kg/m^3	ρ_f
Production Near-Well Pressure Head	-	P_4	Fracture Radius	275 m	R_f
Fracture Net Pressure	-	P_n	Well Depth	5000 m	D
Fracture Critical Pressure	0.1 MPa	P_c	Number of Production Wells	2 wells	n_p
Injection Near-Well Pressure Head	-	P_3	Number of Hydraulic Fractures	50 fractures	n_f
Injection Bottomhole Pressure Head	-	P_2	Number of Fracture Strands	2 strands	n_s
Injection Wellhead Pressure Head	-	P_1	Young's Modulus	60 GPa	E
Well Hydraulic Roughness	80	f	Poisson's Ratio	0.30	ν
Well Hydraulic Diameter	0.1016 m (8")	$2R_w$	Rock Density	2700 kg/m^3	ρ_r
Well Spacing	250 m	L	Passive Earth Coefficient	0.5	K
Fracture Linear Flow Length	167 m	l	Propped Fracture Permeability	1e^{-11} m^2	k
Fracture Radial Flow Length	42 m	r	Propped Fracture Aperture	0.001 m	Ψ_0
Hydraulic Aperture Coefficient	0.95	N	Propped Fracture Compressibility	3.0e-8 Pa^{-1}	α

4. ANALYSIS

The behavior of injection pressure as a function of injection rate is up first for discussion (Figure 2). With our model, we anticipate that the hydraulic fracture will open in tension when the entry pressure into the fracture first exceeds the minimum principal stress. The fracture net pressure can then rise slightly above this value, up to 0.1 MPa positive net pressure, before the fracture will grow. Meanwhile, flow from the production well relieves this pressure in a stable way as long as the frictional losses through the production well do not induce too much back pressure in the bottom of the production well. For reference, the fracture's hydraulic conductivity in this model is 10^{-14} m^2-m (33 mD-ft) with a proppant permeability of 10^{-11} m^2 (10 D) and zero-stress propped aperture of 0.001 m (1 mm).

Finding exact solutions for steady-state flow during injection at rates between the moment of fracture opening and the caging limit is not trivial. To be more accurate, the solutions in this flow regime are highly unstable, both numerically and physically. Lab and field evidence have shown that this pressure trends towards the critical net pressure within the facture and then drops abruptly as the fluid enters the production well (Frash et al., 2025). At EGS Collab, video showed this effect as a fine misting spray entering the well, which suggests a nozzle flow effect where the inertia of the fluid holds a key role in how the pressure drops so abruptly (Fu et al., 2021). Computationally, the pressure drop through the highly conductive open fractures is extremely small, meaning that double-precision floating point addition will simply treat the pressure drop as zero (i.e., a rounding error). This creates a dilemma, especially given the scale and duration of EGS projects. Here we assume the behavior indicated by measurements where the fracture held open at its critical net pressure.

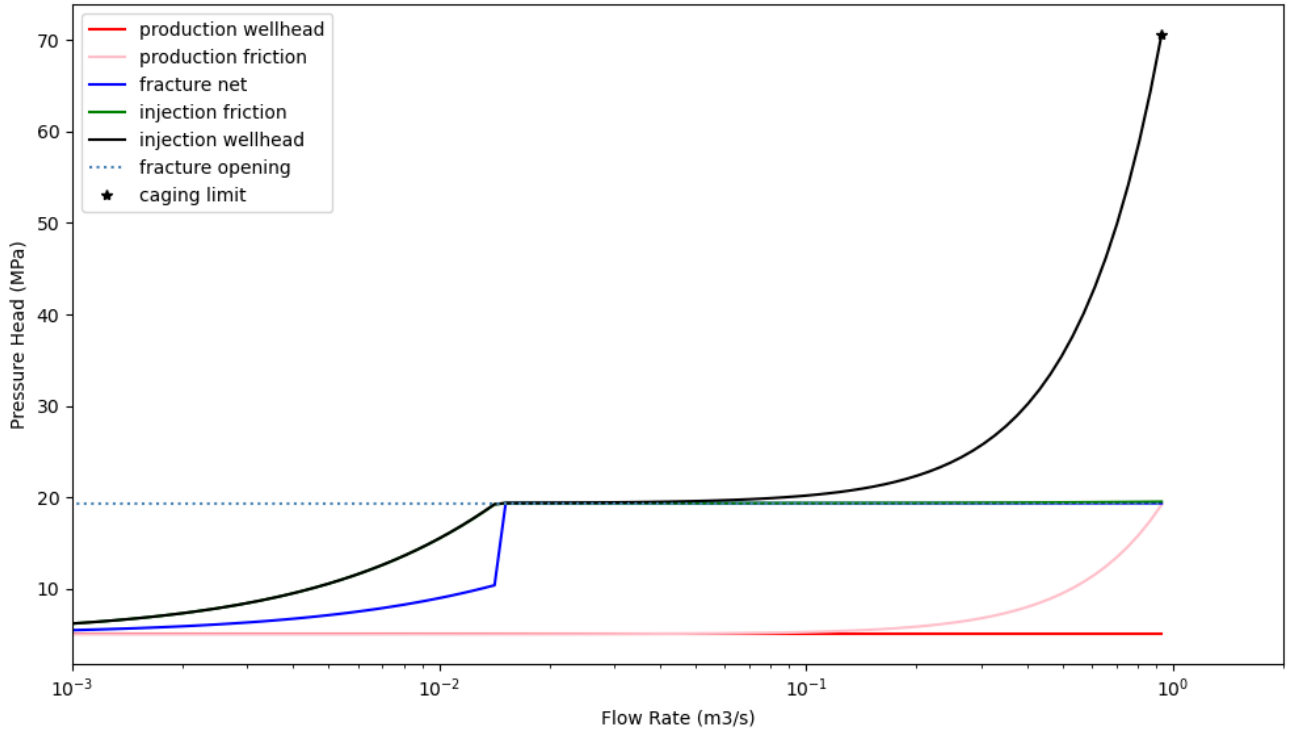

Figure 2: Pressure head with a ground level datum showing building frictional losses across the sand propped fracture until it opens due to the bottomhole injection pressure exceeding the closure stress. With increasing injection rate rise, fracture net pressure can remain stable without fracture growth, up until the back pressure from frictional losses in the production wells becomes too high and the fracture net pressure can no-longer stay below its critical value for growth.

Next, we can deviate the model parameters away from the base case (Figure 3). Key parameters to modify include proppant permeability, well depth, and well diameter. Increasing the proppant permeability delays the onset of fracture opening to higher injection rates because the fluid can more easily flow through the fractures while they remain closed. Increasing the depth causes the fracture opening pressure to increase, meaning more pumping horsepower is needed. Increasing the well diameter increases the maximum injection rate that can be caged and decreases injection pressure as a function of flow rate, which will reduce parasitic losses during EGS production.

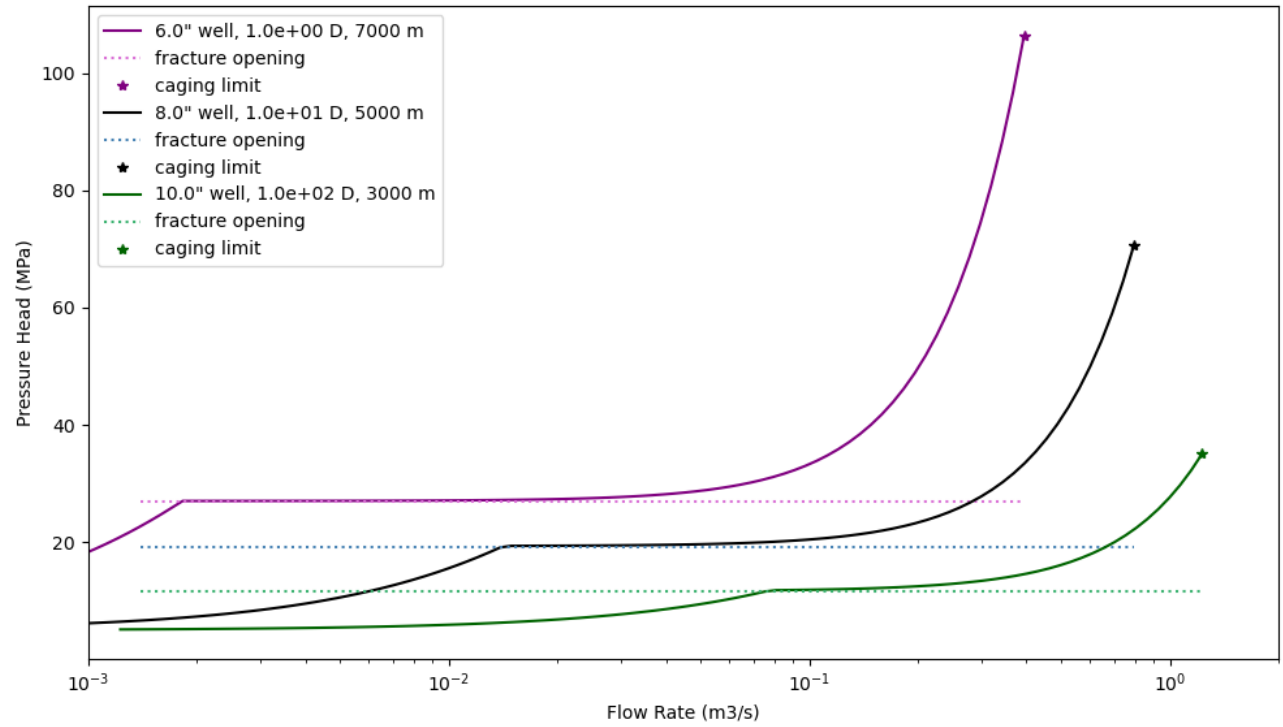

Figure 3: Effect of changing proppant permeability, well depth, and well diameter on injection pressure as a function of rate.

Building on this foundation, we can now recast this information into a mock injection timeseries (Figure 4). This presents a familiar view to anyone who has done such a test before, whether in the lab or field. Here, we also calculate injectivity and inferred fracture permeability by omitting the known fracture permeability and propped aperture. Key details to note from this figure are detailed below.

1. Injection wellhead pressure deviates substantially from the injection bottomhole pressure at high injection rates, despite the bottomhole pressure being constant when a fracture is hydropropped. To confirm hydropropping in field data, or to verify that the injection pressure is less than the frac gradient, the injection wellhead pressure must be corrected to estimate bottomhole pressure. Then, the signature of hydropropping is a negligible increase in pressure with increasing flow rate.
2. With facture caging (CGS) using two or more production wells, high-rate injection can be sustained without losing much of the injected fluid, if the wells have a large enough diameter to mitigate the downhole pressure buildup.
3. Injectivity and inferred fracture permeability have questionable value when applied to step-rate injection data if the injection exceeds the fracture opening pressure. Here, the actual fracture's hydraulic aperture is stable at 0.00016 m (0.16 mm) when closed and effectively infinite (>2 mm) when hydropropped. Meanwhile, injectivity and inferred permeability are proportional to the injection rate after the fracture opens. When used in this case, the injectivity and inferred permeability are not providing any meaningful information about the reservoir properties. Relatedly, that increased permeability is not permanent.

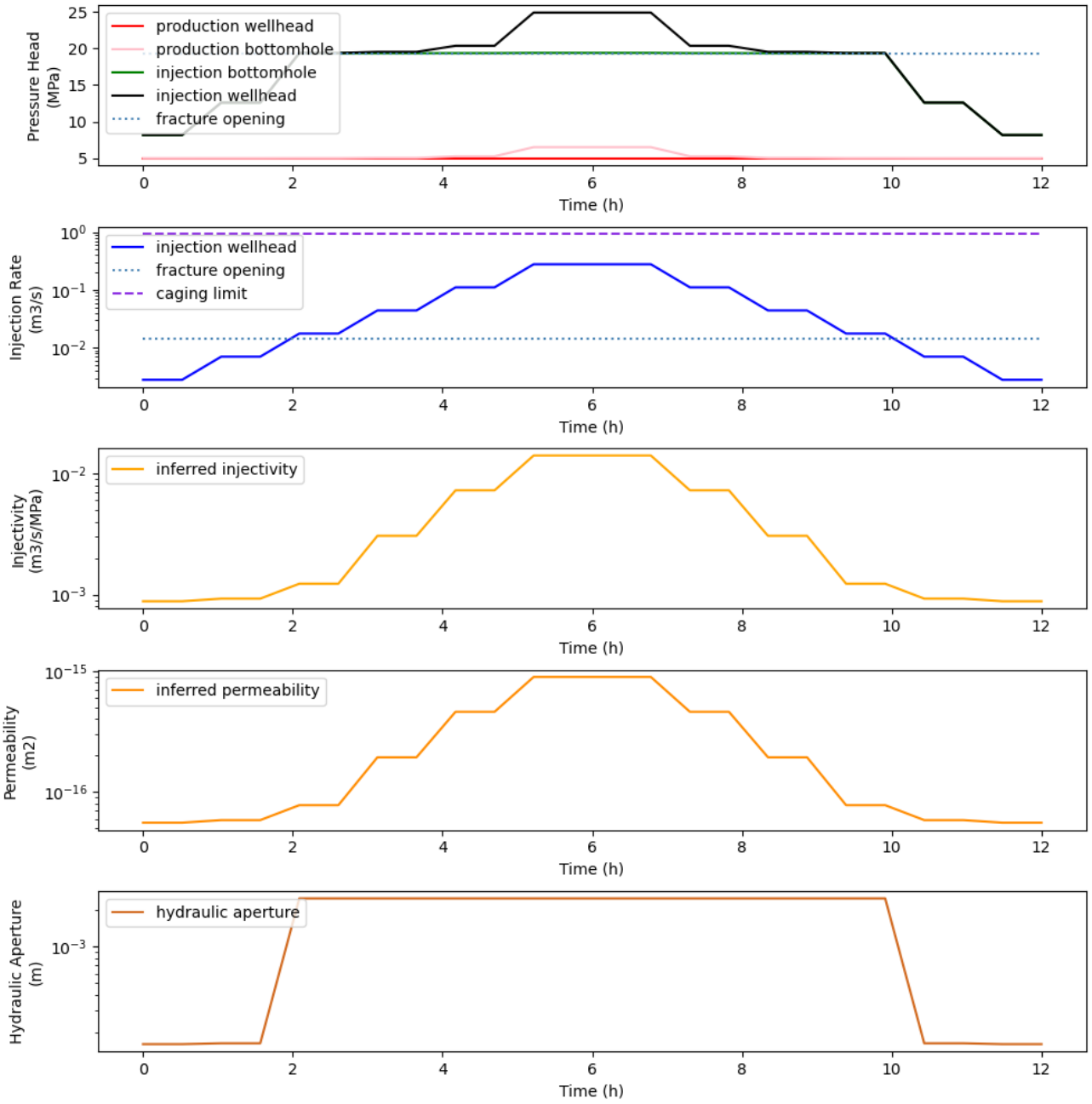

Figure 4: Mock injection timeseries for step-rate injection with stress-dependent fracture aperture and well friction.

In the above plot (Figure 4), injectivity (I) and inferred permeability (k') are calculated using a field relevant approach where the aperture of the fracture is unknown, so an arbitrary length of the injection well is used instead (b; 500 m). Likewise, an arbitrary fluid invasion radius is also used (r; 500 m). Granted, these estimates can be converted to other values if the arbitrary values are known. This omission is not avoidable due to the lack of measurement tools that are capable of measuring fracture aperture anywhere except immediately along the wellbore. Inversion models offer an alternative method to estimate permeability, but these also have issues with non-uniqueness due to interdependency between permeability, porosity, compliance, and hydraulic diffusivity.

$$I = \frac{\Delta Q}{\Delta P_i} \tag{14}$$

$$k' = \frac{\mu I}{2\pi b} \ln\left(\frac{r}{R_w}\right) \tag{15}$$

6. CONCLUSIONS

In this study, we use a conceptual model of a three-well EGS reservoir with 50 fractures to elucidate injection rate and pressure behavior. The model and its assumptions are based on laboratory and field observations, most notably that hydropropped fractures (i.e., fractures held open by fluid pressure) tend to sustain high-pressure throughout even while being actively drained by production wells. The results from this model show how increasing proppant permeability will delay the onset of hydropropping to enable commercial-rate injection (e.g., >0.04 m^3/s) at pressures less than the frac gradient (i.e., fracture opening pressure). They also show that increasing EGS reservoir depth will bring extra challenges for sustaining a productive reservoir because of the stress-driven compression of proppants and increased pressure demand for stimulation and/or hydropropping. To combat these negatives, larger injection and production wells can help to lower injection pressure requirements and can help to improve our ability to prevent fracture growth via fracture caging. Finally, the results show why bottomhole pressure corrections are essential for interpreting the onset of hydropropping (e.g., negligible pressure increase with increasing injection rate). Relatedly, the results show how calculated injectivity and inferred fracture permeability that are sometimes estimated from injection wellhead data can be highly misleading, to the point that they may reveal nothing of value about the reservoir's properties. Armed with this improved understanding, field data from EGS injection wells can be better interpreted as we collectively seek the most viable option for developing hot dry rock geothermal resources.

ACKNOWLEDGEMENTS

This work is supported by Department of Energy (DOE) Basic Energy Sciences under FWP LANLE3W1. Additional support was provided by the Los Alamos National Laboratory's Laboratory Directed Research and Development – Exploratory Research program (LDRD-ER-20220175ER) and the DOE Geothermal Technologies Office (GTO) funded project – Geothermal Limitless Approach to Drilling Efficiencies (GLADE; DE-EE0010444) led by Oxy USA, Inc. I am grateful for this funding provided by DOE and LANL. The views expressed herein do not necessarily represent the views of the U.S. Department of Energy of the United States Government.

REFERENCES

Brown, D.W., Duchane, D.V., Heiken, G., Hriscu, V.T.: Mining the Earth's Heat: Hot Dry Rock Geothermal Energy, Springer, (2012).

Fisher, K., Warpinski, N.: Hydraulic-Fracture-Height Growth: Real Data, SPE Production and Operations, 27 (1), 8-19, (2012).

Frash, L.P., Fu, P., Morris, J., Gutierrez, M., Neupane, G., Hampton, J., Welch, N.J., Carey, J.W., Kneafsey, T.: Fracture Caging to Limit Induced Seismicity, Geophysical Research Letters, 48 (1), e2020GL090648, (2021).

Frash, L.P., Gutierrez, M., Hampton, J., Hood, J.: Laboratory simulation of binary and triple well EGS in large granite blocks using AE events for drilling guidance, Geothermics, 55, 1-15, (2015).

Frash, L.P., Hampton, J., Gutierrez, M., Tutuncu, A., Carey, J.W., Hood, J., Mokhtari, M., Huang, H., Mattson, E.: Patterns in complex hydraulic fractures observed by true-triaxial experiments and implications for proppant placement and stimulated reservoir volumes, Journal of Petroleum Exploration and Production Technology, 9, 2781-2792, (2019).

Frash, L.P., Meng, M., Li, W.: Validation of fracture caging to contain hydraulic fractures: timeseries, videos, and model script. Zenodo, doi.org/10.5281/zenodo.8274273, (2023).

Frash, L.P., Meng, M., Li, W., K C, B., Madenova, Y.: Exploring the physical limits of hydraulic fracture caging to forecast its feasibility for geothermal power generation, Renewable Energy, 241, 122364, (2025).

Fu, P., Schoenball, M., Ajo-Franklin, J.B., Chai, C., Maceira, M.: Close Observation of Hydraulic Fracturing at EGS Collab Experiment 1: Fracture Trajectory, Microseismic Interpretations, and the Role of Natural Fractures, Journal of Geophysical Research: Solid Earth, 126, e2020JB020840, (2021).

Geertsma, J., De Klerk, F.: A Rapid Method of Predicting Width and Extent of Hydraulically Induced Fractures, Journal of Petroleum Technology, 21 (12), 1571-1581, (1969).

Hubbert, M.K., Willis, D.G.: Mechanics of Hydraulic Fracturing, AIME Petroleum Transactions, 210, (1957).

Jeppson, R.W.: Steady flow analysis of pipe networks: an instructional manual, Reports, Paper 300, (1974).

Kneafsey, T. The EGS Collab project: Outcomes and lessons learned from hydraulic fracture stimulations in crystalline rock at 1.25 and 1.5 km depth, Geothermics, 126, 103178, (2025).

Lecampion, B., Bunger, A., Zhang, X.: Numerical methods for hydraulic fracture propagation: A review of recent trends, Journal of Natural Gas Science and Engineering, 49, 66-83, (2018).

Li, W., frash, L.P., Welch, N.J., Carey, J.W., Meng, M., Wigand, M.: Stress-dependent fracture permeability measurements and implications for shale gas production, Fuel, 290, 119984, (2021).

Madenova, Y., Frash, L.P., Li, W., Meng, M., K C, B., Hampton, J., Xiong, Q., Viswanathan, H.S.: Fracture caging in a lab fault to prevent seismic rupture during fluid injection, Geothermics, 126, 103206, (2025).

Meng, M., Frash, L.P., Li, W., Welch, N.J., Carey, J.W., et al.: Hydro-Mechanical Measurements of Sheared Crystalline Rock Fractures With Applications for EGS Collab Experiments 1 and 2, Journal of Geophysical Research: Solid Earth, 127, e2012JB2300, (2022).

Norbeck, J.H., Lattimer, T.M.: Commercial-Scale Demonstration of a First-of-a-Kind Enhanced Geothermal System, Earth ArXiv, https://doi.org/10.31223/X52X0B, (2023).

Nordgren, R.P.: Propagation of a Vertical Fracture, Society of Petroleum Engineers Journal, 12 (4): 306-314, (1972).

Perkins, T., Kern, L.: Widths of Hydraulic Fractures. Journal of Petroleum Technology, 222, 937-949, (1961).

Valko, P., Economides, M.J.: Hydraulic Fracture Mechanics, Wiley, ISBN: 978-0-471-95664-8, (1996).

Welch, N.J., Carey, J.W., Frash, L.P., Hyman, J.D., et al.: Effect of Shear Displacement and Stress Changes on Fracture Hydraulic Aperture and Flow Anisotropy, Transport in Porous Media, 141, 17-47, (2022).

Witherspoon, P.A., Wang, J.S.Y., Iwai, K., Gale, J.E.: Validity of cubic law for fluid flow in a deformable rock fracture, Water Resources research, 16: 1016-1024, (1980).

Yen, R.T.: Radial flow between two parallel discs, Kansas State University, Department of Applied Mathematics, (1962).

Zoback, M.D.: Reservoir Geomechanics, Cambridge University Press, ISBN: 978-0521146197, (2010).